On the Control of the Resonant Converter: A Hybrid-Flatness Approach

Hebertt Sira-Ramírez and Ramón Silva-Ortigoza

Departamento de Ingeniería Eléctrica
CINVESTAV-IPN
Avenida IPN, 2508, Col. San Pedro Zacatenco, A.P. 14740
México, D.F., México.
e-mail:hsira@mail.cinvestav.mx
ramsilv@prodigy.net.mx
Phone: 52-5747-3800x-6308,6311. Fax: 52-5747-3866

Abstract

In this article we show that the series resonant DC/DC converter, which is a hybrid system, is piecewise differentially flat with a flat output which is invariant with respect to the structural changes undergone by the system evolution. This fact considerably simplifies the design of a switching output feedback controller that can be essentially solved by linear techniques. Flatness clearly explains all practical issues associated with the normal operation of the converter.

1 Introduction

In aim of the present paper is to present an alternative approach to the regulation problem of a popular DC/DC power converter, known as the *series resonant converter* (*SRC*), from the combined perspective of differential flatness and hybrid systems. The converter is a variable structure system with a linear controllable model in each one of the two *locations*, or regions, of the systems hybrid state space. On each constitutive location of the corresponding hybrid automaton the system is thus represented by a *flat* system. The flat output expression of the system, in terms of the state variables, is distinctively marked by the hybrid character of the system. However, the differential relation existing between the flat output and the control input is *invariant* throughout the set of locations. By resorting to flatness, one clearly shows that the circuit variables which are required to achieve resonance (i.e., sinusoidal oscillatory behavior) also exhibit invariant differential parameterizations, in terms of the flat output. These two facts considerably simplify the hybrid controller design problem for both the *start up* phase and the *steady state energy* set point regulation phase of the converter. The regulation of the *steady state oscillations* entitle switchings on a hyperplane whose synthesis requires knowledge of the resonant state variables. Furthermore, by designing a prototype, we show explicitly that ours theoretical and experimental results are in good agreement.

2 The series resonant DC/DC power converter

Resonant converters have been the object of sustained interest throughout the last two decades. Roughly speaking, the controller design for such hybrid systems has been approached from different viewpoints including: an approximate DC viewpoint, a phase plane approach, averaging methods defined on phasor variable methods and, more recently, from a passivity based approach.

Approximate analysis, based on DC considerations, was undertaken in Vorpérian and Cúk [1], [2]. These tools are rather limited given the hard nonlinear nature of the converter. Control strategies based on state variable representations were initiated in Oruganti and Lee in [3], [4]. These techniques were clearly explained later, on a simplified converter model, in Rossetto [5]. An optimal control approach was developed in Sendanyoye *et al* [6] and a similar approach was reported in the work of Oruganti *et al* [7]. Several authors have also resorted to either exact or approximate discretization strategies as in Verghese *et al* [8] and in Kim *et al* [9]. A phasor transformation approach was provided in the work of Rim and Cho [10], which is specially suited for DC to DC conversion. An interesting averaging method, based on local Fourier analysis, has been presented in an article by Sanders *et al* [11]. These frequency domain approximation techniques have also found widespread use in other areas of power electronics. Using this approach, approximate schemes relying on Lyapunov stability analysis and the passivity based control approach, have been reported, respectively, in the works of Stankovic *et al* [12] and Escobar [13].

Our approach is fundamentally based in the concept of *differential flatness* introduced ten year ago in [14] (see also [15]). The flatness property, exhibited by many systems of practical interest, is here exploited to obtain, from its simple linear dynamics, suitable estimates of the converter state variables by means of linear design techniques.

3 The resonant DC/DC converter nonlinear model

3.1 The converter's nonlinear model

In Figure 1 we show a simplified nonlinear circuit representing the series resonant DC/DC power converter. A direct computation shows that the controlled nonlinear differential equations modelling the circuit are given by [12]

$$\begin{aligned} L\frac{di}{dt} &= -v - v_o sign\,(i) + E\,(t) \\ C\frac{dv}{dt} &= i \\ C_o\frac{dv_o}{dt} &= abs\,(i) - \frac{v_o}{R} - I_o \end{aligned} \tag{3.1}$$

where v and i are, respectively, the series capacitor voltage and the inductor current in the resonant series tank, while v_o is the output capacitor voltage feeding both the load R and the sink current I_o which, for simplicity, we assume to be of value zero. The input to the system is $E\,(t)$, which is usually restricted to take values in the discrete set $\{-E, E\}$ where E is a fixed given constant.

The objective is to attain a nearly constant voltage across the load resistance R on the basis of the rectified, and low-pass filtered, sinusoidal inductor current signal internally generated by the

system in the L, C series circuit with the suitable aid of the amplitude restricted control input signal.

Defining the scaling state space and time transformation,

$$\begin{pmatrix} z_1 \\ z_2 \\ z_3 \end{pmatrix} = \begin{pmatrix} \frac{1}{E}\sqrt{\frac{L}{C}} & 0 & 0 \\ 0 & \frac{1}{E} & 0 \\ 0 & 0 & \frac{1}{E} \end{pmatrix} \begin{pmatrix} i \\ \upsilon \\ \upsilon_o \end{pmatrix}, \qquad \tau = \frac{t}{\sqrt{LC}} \tag{3.2}$$

One readily obtains the following *normalized* model of the resonant circuit equations (3.1).

$$\begin{aligned} \dot{z}_1 &= -z_2 - z_3 sign\,(z_1) + u \\ \dot{z}_2 &= z_1 \\ \alpha \dot{z}_3 &= abs\,(z_1) - \frac{z_3}{Q} \end{aligned} \tag{3.3}$$

where, abusing the notation, the symbol: " $\dot{}$ " now represents derivation with respect to the scaled time, τ. The variable, u, is the normalized control input, necessarily restricted to take values in the discrete set, $\{-1, +1\}$. The parameter Q, defined as $Q = R\sqrt{C/L}$, is known as the *quality factor* of the circuit, while the constant, α, is just the ratio, $\alpha = C_o/C$.

The normalized resonant converter may then be represented as the *hybrid automaton* shown in Figure 2 (see Van der Schaft and Schumacher in [16]).

3.2 Differential flatness of the hybrid converter

We propose to view the normalized converter system dynamics (3.3) as constituted by a *hybrid* combination of two linear controllable (i.e., differentially flat) systems, each one characterized by a corresponding flat output. Consider then the following pair of controllable linear systems, derivable from the system model for the instances in which $z_1 > 0$ and $z_1 < 0$, respectively.

for $z_1 > 0$

$$\begin{aligned} \dot{z}_1 &= -z_2 - z_3 + u \\ \dot{z}_2 &= z_1 \\ \alpha \dot{z}_3 &= z_1 - \frac{z_3}{Q} \end{aligned}$$

for $z_1 < 0$

$$\begin{aligned} \dot{z}_1 &= -z_2 + z_3 + u \\ \dot{z}_2 &= z_1 \\ \alpha \dot{z}_3 &= -z_1 - \frac{z_3}{Q} \end{aligned}$$

Indeed, on each state space *location* the system is constituted by a controllable and, hence, differentially flat system. As a result, there exists, in each case, a flat output y which is a linear combination of the state variables. Such outputs allow for a complete differential parameterization

of each local representation of the system. The flat output variables are given by,

$$y = z_2 - \alpha z_3 \quad ; \quad \text{for } z_1 > 0$$
$$y = z_2 + \alpha z_3 \quad ; \quad \text{for } z_1 < 0$$

which have the physical meaning, respectively, of being proportional to the difference and the sum of the instantaneous stored charges in the series capacitor, C, and the output capacitor, C_o.

One readily obtains the following differential parameterization of the constitutive system variables in each case

for $z_1 > 0$

$$\begin{aligned} z_3 &= Q\dot{y} \\ z_2 &= y + \alpha Q\dot{y} \\ z_1 &= \dot{y} + \alpha Q\ddot{y} \\ u &= \alpha Q y^{(3)} + \ddot{y} + Q\,(1+\alpha)\,\dot{y} + y \end{aligned}$$

for $z_1 < 0$

$$\begin{aligned} z_3 &= -Q\dot{y} \\ z_2 &= y + \alpha Q\dot{y} \\ z_1 &= \dot{y} + \alpha Q\ddot{y} \\ u &= \alpha Q y^{(3)} + \ddot{y} + Q\,(1+\alpha)\,\dot{y} + y \end{aligned}$$

The key observations, on which our control approach is based, are the following:

- The differential parameterizations associated with the flat outputs lead to the *same* differential relation between the flat output, y, and the control input u. In other words, independently of the region of the state space of the underlying hybrid system, the flat output satisfies the dynamics,
$$\alpha Q y^{(3)} + \ddot{y} + Q\,(1+\alpha)\,\dot{y} + y = u \tag{3.4}$$
- The normalized series capacitor voltage, z_2, and the normalized inductor current, z_1, (i.e., the *resonant variables*) also exhibit the *same* parameterizations in terms of the corresponding flat output.
$$z_2 = y + \alpha Q\dot{y}, \qquad z_1 = \dot{y} + \alpha Q\ddot{y}$$
These representations are, therefore, invariant with respect to the structural changes undergone by the system.

4 Design of a feedback control strategy

The operation of the series resonant converter undergoes two distinctive phases. The first one is the *start up* phase in which the converter's total stored energy is increased from the value zero towards a suitable level. The second phase is the *steady oscillation* phase in which the resonant condition is regulated to produce a desired resonant voltage amplitude value or, alternatively, an approximately constant stored energy set-point level. Each phase requires of a different feedback controller. Below, we exploit flatness to deal with the two control design phases. We assume throughout that all the variables, are measurable.

4.1 The *start up* feedback controller

The ideal control objective is to induce a sinusoidal behavior on the voltage variable z_2. The relation (3.4), reveals that the variable z_2, coinciding everywhere with the quantity $y + \alpha Q\dot{y}$, satisfies,

$$\frac{d^2}{d\tau^2}(y + \alpha Q\dot{y}) + (y + \alpha Q\dot{y}) + Q\dot{y} = u \tag{4.1}$$

A perfect sinusoidal behavior for the voltage, z_2, would imply that the control input u should exactly cancel the term, $Q\dot{y} = z_3 sign z_1$, so as to render a closed loop dynamics represented by the ideal oscillator: $\ddot{z}_2 + z_2 = 0$. Given the discrete-valued character of $u \in \{-1, +1\}$, such a cancellation is not possible. Thus, at best, the control strategy may be specified as,

$$u(z_1) = sign z_1 = sign(\dot{y} + \alpha Q\ddot{y}) \tag{4.2}$$

It is clarifying to see the effect of the proposed feedback law on the total normalized stored energy of the system, defined as

$$W(z) = \frac{1}{2}\left(z_1^2 + z_2^2 + \alpha z_3^2\right)$$

The time derivative of the normalized stored energy, i.e., the closed loop normalized instantaneous power, is given by

$$\dot{W}(z) = u(z_1) z_1 - \frac{z_3^2}{Q} = |z_1| - \frac{z_3^2}{Q} \tag{4.3}$$

The stored energy thus grows while the condition:

$$|z_1| > \frac{z_3^2}{Q} \tag{4.4}$$

is valid, and it decreases otherwise (see Figure 3). Since the variables of the converter are all started from the zero value (i.e., from the zero energy level), the devised hybrid feedback control law (4.2) is clearly useful in increasing the energy of the converter up to a certain desired level.

4.2 The steady state feedback regulator

Notice that if we insist in using the control strategy (4.2) for an indefinite period of time, the resonant variables will stabilize to an approximately sinusoidal steady state behavior, characterized by fixed maximum amplitude signals. We, thus, loose the possibilities of decreasing, or further increasing, at will, both the operating energy level of the converter and the corresponding amplitudes of the resonant variables. This would mean that the output voltage also remains approximately constant. Therefore, the control law (4.2) should be suitably modified, right after a reasonable intermediate level of stored energy is reached. The modification should be geared to recover some degree of set point regulation around a prespecified operating energy level reference set-point.

A regulation strategy for the *steady state oscillation* phase consists in suitably changing from the switching *start up* controller to a second switching controller that is capable of sustaining the achieved oscillatory behavior of the resonant variables. This may be accomplished by choosing a switching hyperplane different to $z_1 = 0$. We propose to use a switching strategy based entirely on the flat output y.

Define $\sigma = z_1 - kz_2 = \alpha Q\ddot{y} + \dot{y} - k\left(y + \alpha Q\dot{y}\right)$, with $k > 0$ being a constant parameter, and consider the switching strategy,

$$u = sign\sigma = sign\left[\alpha Q\ddot{y} + \dot{y} - k\left(y + \alpha Q\dot{y}\right)\right] \tag{4.5}$$

It is easy to show that the switching policy (4.5) produces a stable oscillation in the reduced phase space $(z_1, z_2) = (\dot{z}_2, z_2)$ whose steady state amplitudes can be now *calibrated* in terms of the design parameter k, representing the slope of the switching line in the plane (z_1, z_2). The differential parameterization provided by flatness also allows for a calibration of the resonant variables amplitudes in terms of k.

5 Simulation and experimental results

In order to evaluate the validity of the proposed controls, these controls are implemented and tested in conjunction with the full-bridge *SRC* operating in resonant frequency.

The following parameters are used in the experimental test bed. The inductance and capacitance in the resonant tank circuit are $L = 1.5mH$, $C = 10.6nF$, respectively. This corresponds to a resonant frequency of $f_r = 40KH$. The capacitor in the output filter is $C_o = 1\mu F$. A commercial dc-voltage source is fixed to $48V$ in order to feed the *SRC* circuit. The robustness of the control laws against disturbances introduced by this source has not been considered here. For the moment, we assume that the dc voltage source provides a constant dc voltage level. The experimental setup neither allows changes in the load resistance, it is 72Ω. The converter was designed to supply $25W$ of power. Finally, the output voltage was designed to supply $42V$. The given parameter values result in $\alpha = 94.34$ and $Q = 0.1914$.

5.1 Simulation results

Now, using relationship between normalized and real time

$$\tau = \frac{t}{\sqrt{LC}} \tag{5.1}$$

we have the following:

$$\tau = \frac{t}{\sqrt{LC}} = \left(2.5078 \times 10^5\right) t \tag{5.2}$$

$$t = \sqrt{LC}\tau = \left(3.9875 \times 10^5\right) \tau \tag{5.3}$$

In simulations we used a sample period $2.5 \times 10^{-7}\ s$, which gives the normalized time

$$\tau = \frac{t}{\sqrt{LC}} = 62.696 \times 10^{-3}.$$

(In this subsection in all the figures $t^* = \tau$.)

Commutation between the two control strategies must be done when (4.4) is violated. However, necessary hardware to verify this condition is huge. Hence, we have used an alternative criterion to commute. From (4.3) we see energy increases while (4.4) is satisfied. Thus, it is simply a matter of time before this condition is violated. We decided to commuted at $t = 50.11\ \mu s$ ($\tau = 12.57$).

Figure 4 shows behavior of state variables, control input, total power and oscillations in the phase plane (z_1, z_2), when *start up* strategy is used alone.

Figure 5 depicts the combined used of *start up* and *steady state oscillation* strategies. This figure was obtained assuming all required state variables used in feedback were measurable. We use the value $k = 1$. Note steady state values of stored energy, corresponding resonant voltage amplitude and resulting output voltage are now inferior to the corresponding ones obtained in Figure 4.

Figure 6 depicts several output voltage responses and power for different values of k. This demonstrates *steady state oscillation* strategy allows to control the steady state value of output voltage and the total stored energy. The corresponding phase plots are shown in Figure 7 for $k = 0, 1, 2, 5$.

5.2 Prototype development

A block diagram is shown in Figure 8. We remark that there are three important blocks:

- *Resonant-rectifier*. It is made up of two components: 1) a *series resonant circuit* and 2) a *rectifier*. The electric diagram is shown in Figure 9.
- *Driver-inverter*. It is made up of two components: 1) a *driver* and 2) an *inverter*. The core of the first one is a IR2110 integrated circuit. It receives two complementary square waves from the *control* block and uses them to appropriately trigger transistors of the *inverter*. The second one consists of four power transistors connected in full-bridge configuration. Figure 10 shows the corresponding electric diagram.
- *Control*. In this block the control strategies are implemented using analog electronics. This receives voltage and current signals (i and v) from the *resonant-rectifier* block. It also includes a delay circuit to avoid short circuits during power transistors commutation in the full-bridge. The electric diagram is shown in the Figure 11.

Resonant-rectifier and *driver-inverter* blocks implementation is well known. See Kazimierczuk and Czarkowski [17] for the former and Mohan *et al*, Steigerwald, and Nelms *et al*, in [18], [19] and [20], for the latter. Hence in what follows we concentrated in the *control* block.

5.3 The control block

In this block we implement the control strategies (4.2) and (4.5) by means of analog electronics. Using (3.2), equations (4.2) and (4.5) can be written as,

$$u(i) = sign(i) \tag{5.4}$$

$$u(i, v) = sign\left[\sqrt{\tfrac{L}{C}}i - kv\right]. \tag{5.5}$$

Control law (5.4) is implemented by using the circuit shown in Figure 11. CT is a current transformer CS4050V−01 (see *www.coilcraft.com*). We have used $R_T = 50\Omega$ which allows to have $1V$ in its terminals for each ampere in the primary winding. In (5.4) possible values of $u(i)$ are $+1$ and -1, meaning on/off, respectively. In Figure 11, $Q_1(t)$ represents $u(i)$, whose only possible values are $12V$ and $0V$ corresponding to $+1$ and -1, respectively.

Implementation of control law (5.5) is done as shown in Figure 11. According to simulations we obtained that υ_C reaches its maximum value is $450V$, which is difficult to measure directly. Hence we use voltage transformer (VT) with ratio $n = \frac{1}{10}$, together with a potentiometer as a tension divisor to have $\nu_x = \frac{1}{40}\upsilon_C$ (see Figure 11). Because of this voltage attenuation we have to do so with current in order to keep correct proportions in (5.5). Hence we have

$$u\left(i,\upsilon\right) = sign\left[9.14i - \tfrac{1}{40}k\upsilon\right] \tag{5.6}$$

In Figure 11, Q_2 represents $u\left(i,\upsilon\right)$ whose only possible values are $12V$ and $0V$ corresponding to $+1$ and -1, respectively.

On the other hand, timer used to *commute* between control strategies (5.4) and (5.6) as well as delay circuit are shown in Figure 13 and Figure 12, respectively. Finally, electric diagram of the whole *control* block is shown in Figure 11 and picture of the whole SRC prototype is shown in Figure 14.

5.4 Experimental results

In this section we present the experimental results achieved in the bank of test this is shown in the Figure 14. We first presented, for the purposes of comparison, the response of the converter to the *start up* feedback strategy applied for an indefinite period of time. In Figure 15 we show the behavior of the state variables, the control input, the total power and the oscillations achieved in the resonant variables phase plane (z_1, z_2). Observe that the experimental and simulated results are in good agreement, see Figures 4.

Figure 16 depicts the *combined start up* and *steady state oscillation* phases of the feedback regulation strategy. The figures also show the trajectory of the applied control input. We use the value $k = 1$. Note that the steady state value of: the power, the resonant voltage amplitude and the resulting output voltage are now inferior to the corresponding ones obtained by the application of the *start up* feedback strategy alone, which are in good agreement with the results shown in Figure 5.

Figure 17 depicts several output voltage responses and of the power for different values of the parameter k.

6 Conclusions

In this article we have presented a flatness based approach for the regulation of a hybrid system represented by the popular *series resonant DC/DC converter*. The system dynamics was shown to be representable as a hybrid automaton undergoing structural changes on the common boundary of two clearly identified regions of the state space. Each one of the constitutive dynamic systems of the automaton happens to be *differentially flat*. The key feature that allows a simple approach to the *star up* and *steady state amplitude oscillation regulation* phases of the converter is constituted by the following facts: 1) The flat output, which, as in almost every case, has a clear physical interpretation, exhibits a controlled dynamics relation which is *invariant* with respect to the system's structural changes. 2) The differential parameterizations of the resonant state variables, placed in terms of the flat output, are also *invariant* with respect to the same structural changes. The practical limitation which is related to fixed control input amplitudes is easily handled by the proposed

approach. The effect of a *bang-bang*, or switching control input is easily analyzable on the flat output linear dynamics.

The approach was illustrated by means of digital computer simulations and experimental results in the developed experimental test bench. Since differences between the simulation values and the measured data are due to the winding resistances of the inductors and transformer, the equivalent series resistance of the capacitors, the junction capacitances of the switching devices and the resistances parasites that are neglected in the analysis. We conclude that the simulated and experimental results that are in good agreement.

References

[1] V. Vorpérian and S. Cúk, "A complete dc analysis of the series resonant converter," *IEEE Power Electronics Specialists Conference Record*, 1982, 85-100.

[2] V. Vorpérian and S. Cúk, "Small signal analysis of resonant converters," *IEEE Power Electronics Specialists Conference Record*, 1983, 269-282.

[3] R. Oruganti and F. C. Lee, "Resonant power processors, Part I: State plane analysis," *Proc. IEEE-IAS 1984 Annual Meeting Conference*, 1984, 860-867.

[4] R. Oruganti and F. C. Lee, "Resonant power processors, Part II: Methods of control," *Proc. IEEE-IAS 1984 Annual Meeting Conference*, 1984, 868-878.

[5] L. Rossetto, "A simple control technique for series resonant converters," *IEEE Transactions on Power Electronics*. 11 (1996), no. 4.

[6] V. Sendanyoye, K. Al-Haddad and V. Rajagopalan, "Optimal trajectory control strategy for improved dynamic response of series resonant converter," *Proc. IEEE-IAS'90 Annual Meeting Conference*, 1990, 1236-1242.

[7] R. Oruganti and F.C. Lee, "Implementation of optimal trajectory control of series resonant converter," *IEEE Power Electronics Specialists Conference Record*, 1987, 451-459.

[8] G. C. Verghese, M. E. Elbuluk, and J. G. Kasskian, "A general approach to sample data modeling for power electronics circuits," *IEEE Transactions on Power Electronics*, 1 (1986), no. 2, 76-89.

[9] M. G. Kim, D. S. Lee and M. J. Youn, "A new state feedback control of resonant converters," *IEEE Transactions on Industrial Electronics*, 38 (1991), no. 3.

[10] C. T. Rim, and G. H. Cho, "Phasor transformation and its application to the DC-AC analyses of frequency phase controlled series resonant converters (SRC)," *IEEE Transactions on Power Electronics*, 5 (1990), no. 2.

[11] S. Sanders, J. M. Noworolski, X. Z. Liu and G. C. Verghese, "Generalized averaging methods for power conversion circuits," *IEEE Transactions on Power Electronics*, 6(1991), no. 2, 251-258.

[12] A. M. Stankovic, D. J. Perrault and K. Sato, "Analysis and experimentation with dissipative nonlinear controllers for series resonant DC-DC Converters," *IEEE Power Electronics Specialists Conference Record*, 1997, 679-685.

[13] G. Escobar, "Sur la commande nonlinéaire des systémes d'electronique de puissnce a commutation, " *PhD Thesis, Université de Paris-Sud UFR Scientifique d'Orsay*, (No. d'ordre 5744) Orsay (France), 1999.

[14] M. Fliess, J. Lévine, P. Martín and P. Rouchon, "Sur les systemes non linéaires différentiellement plats," *C.R. Acad. Sci. Paris* , Série I, Mathématiques, 315 (1992), 619-624.

[15] M. Fliess, J. Lévine, Ph. Martín and P. Rouchon, "A Lie-Bäcklund approach to equivalence and flatness," *IEEE Transactions on Automatic Control*, 44 (1999), no. 5, 922-937.

[16] A. J. van der Schaft and J. M. Schumacher, "An Introduction to Hybrid Dynamical Systems," London, Springer-Verlag, 2000, 6-14.

[17] M. K. Kazimierczuk and D. Czarkowski, "Resonant Power Converters," John Wiley & Sons Inc, 1995.

[18] N. Mohan, T. M. Undeland and W. P. Robbins, "Power Electronics: Converters, Applications and Design," New York, John Wiley & Sons, 1989, 211-258.

[19] R. Steigerwald, "A Comparison of half-bridge resonant converter topologies," *IEEE, Transactions on Power Electronics*, 3 (1998), no. 2, 174-182.

[20] R. M. Nelms, T. D. Jones and M. C. Cosby, "A comparison of resonant inverter topologies for HPS lamp ballast," *Annual Meeting of the Industry Applications Society IAS'93*, 3 (1993), 2317-2322.

[21] R. J. Tocci, "Sistemas Digitales: Principios y Aplicaciones," México, Prentice Hall Hispanoamericana, 1993.

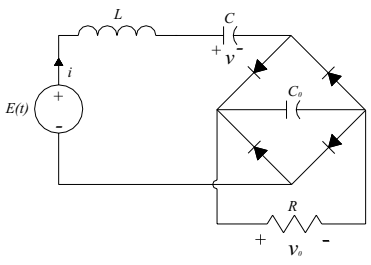

Figure 1: The series resonant converter.

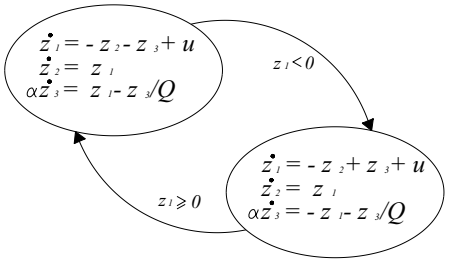

Figure 2: The normalized resonant converter as a hybrid automaton.

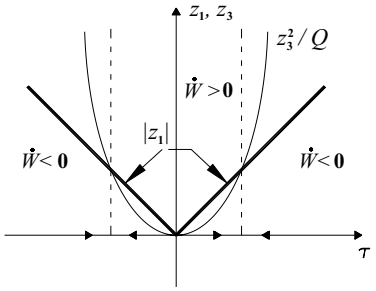

Figure 3: Effect of *start up* switching strategy on energy rate.

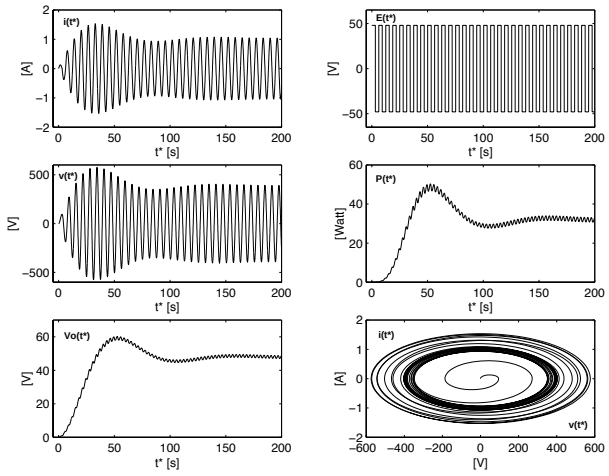

Figure 4: Closed loop responses for the *start up* feedback strategy alone.

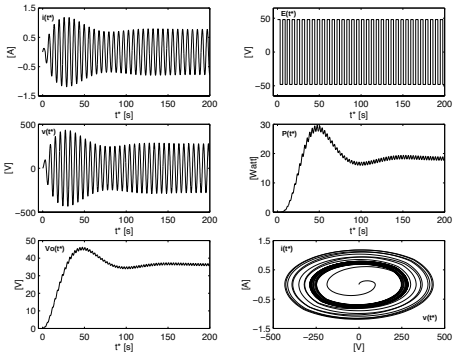

Figure 5: Responses for the *composite start up* and *steady state oscillation* control strategies, $k = 1$.

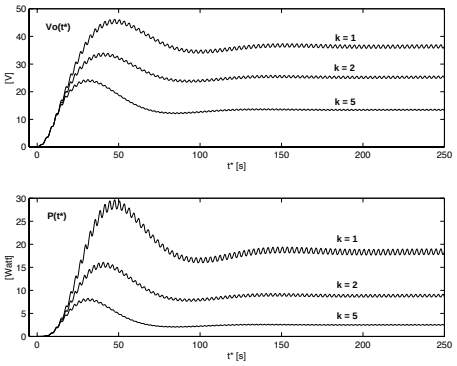

Figure 6: Output voltage and stored energy for $k = 1, 2$ and 5.

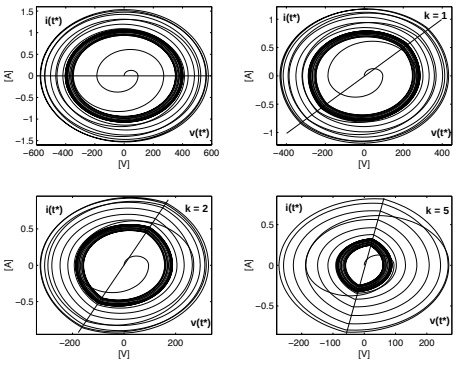

Figure 7: Phase plots for $k = 0, 1, 2$ and 5.

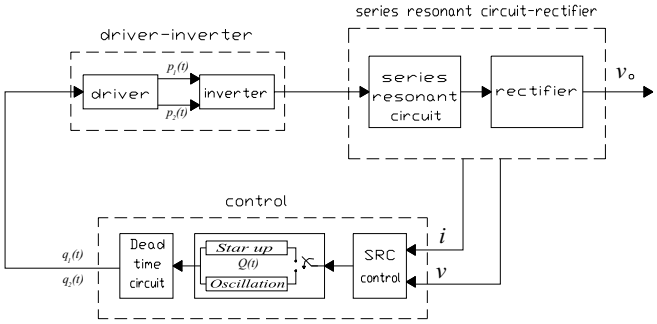

Figure 8: Diagram block of the *SRC* implemented.

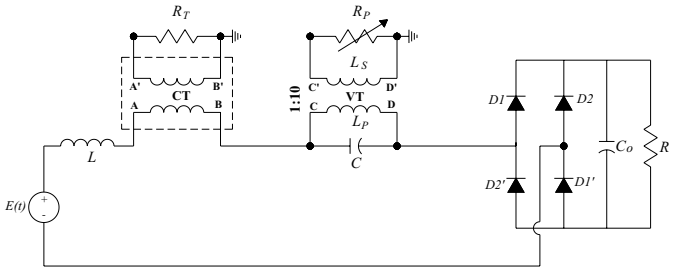

Figure 9: Electric circuit of the *resonant-rectifier* block.

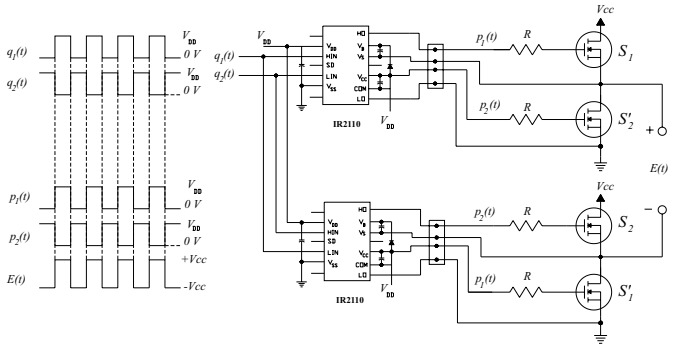

Figure 10: Electric circuit of the *driver-inverter* block.

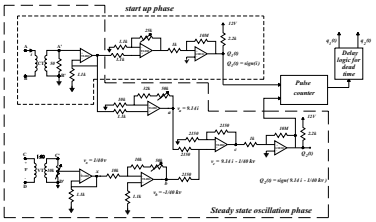

Figure 11: Electric circuit of the *control* block.

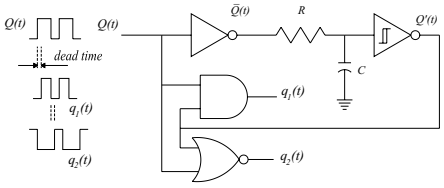

Figure 12: Delay logic for dead time in complementary switch signals.

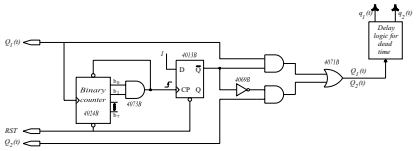

Figure 13: Electric circuit of the pulse counter.

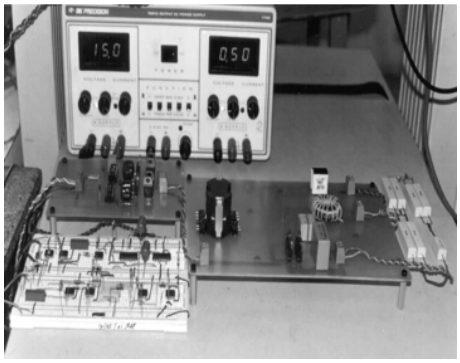

Figure 14: Picture of the developed experimental test bench.

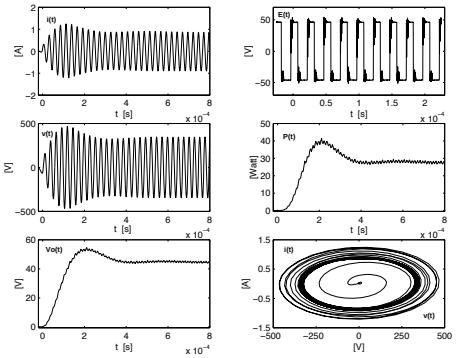

Figure 15: Experimental results: Closed loop for the *start up* feedback strategy alone.

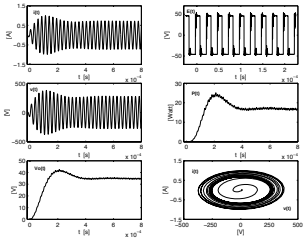

Figure 16: Experimental results: Closed loop responses for the to *composite start up* and *steady state oscillation* control strategies, $k = 1$.

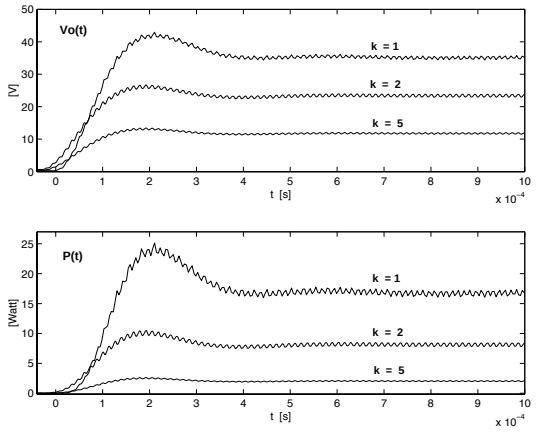

Figure 17: Experimental results: Output voltage and stored energy for $k = 1, 2$ and 5.